

# Nanostructures by Self-Assembling Peptide Amphiphile as Potential Selective Drug Carriers

Antonella Accardo,<sup>1</sup> Diego Tesaro,<sup>1</sup> Gaetano Mangiapia,<sup>2</sup> Carlo Pedone,<sup>1</sup> Giancarlo Morelli<sup>1</sup>

<sup>1</sup> Department of Biological Sciences, CIRPeB University of Naples "Federico II", & IBB CNR, Via Mezzocannone 16, 80134 Naples, Italy

<sup>2</sup> Department of Chemistry, University of Naples "Federico II", Via Cinthia, 80126 Naples, Italy

Received 18 October 2006; revised 24 November 2006; accepted 5 December 2006

Published online 8 December 2006 in Wiley InterScience (www.interscience.wiley.com). DOI 10.1002/bip.20648

## ABSTRACT:

The self-assembling behavior, at physiological pH, of the amphiphile peptide (C18)<sub>2</sub>L5CCK8 in nanostructures is reported. Stable aggregates presenting a critical micellar concentration of  $2 \times 10^{-6}$  mol kg<sup>-1</sup>, and characterized by water exposed CCK8 peptide in  $\beta$ -sheet conformation, are obtained. Small angle neutron scattering experiments are indicative for a 3D structure with dimensions  $\geq 100$  nm. AFM images confirm the presence of nanostructures. Fluorescence experiments indicating the sequestration of pyrene, chosen as drug model, and the anticancer Doxorubicin within the nanostructures are reported.

© 2006 Wiley Periodicals, Inc. *Biopolymers (Pept Sci)* 88: 115–121, 2007.

**Keywords:** peptide amphiphile; nanostructures; drug delivery; SANS; circular dichroism

This article was originally published online as an accepted preprint. The "Published Online" date corresponds to the preprint version. You can request a copy of the preprint by emailing the *Biopolymers* editorial office at [biopolymers@wiley.com](mailto:biopolymers@wiley.com)

Correspondence to: Giancarlo Morelli, Department of Biological Sciences, CIRPeB University of Naples "Federico II", & IBB CNR, Via Mezzocannone 16, 80134 Naples, Italy; e-mail: [gmorelli@unina.it](mailto:gmorelli@unina.it)

Contract grant sponsor: European Molecular Imaging Laboratories Network (EMIL)

Contract grant sponsors: the European Commission, NMI3

Contract grant number: RII3-CT-2003-505925



© 2006 Wiley Periodicals, Inc.

## INTRODUCTION

Peptide amphiphile (PA) molecules, consisting of a hydrophilic peptide sequence covalently linked to a hydrophobic moiety, self-assemble in highly ordered, one dimensional cylindrical nanostructures.<sup>1–7</sup> In these supramolecular structures the hydrophobic moieties remain in the nanostructure interior space by hydrophobic collapse, while the hydrophilic peptide sequences are consequently displayed on the nanostructure surface, with orientation order resulting from  $\beta$ -sheet formation during the self-assembling process. In this sense, these nanostructures differ from ordinary cylindrical micelles, which typically have less ordered hydrophobic and hydrophilic compartments. The peptide moiety, remaining on periphery of the nanostructure, enables different chemical and biological functionalities. It has been shown that this kind of nanostructures is able to template the crystallographic orientation in hydroxyapatite mineralization<sup>1</sup> and to promote the selective differentiation of neural progenitor cells.<sup>4</sup> Moreover PA nanostructures functionalized with bioactive sequences exhibit exceptional properties, including the ability to reach in a selective way a biological target,<sup>6</sup> or allowing formation of pores in membranes.<sup>7</sup>

The self-assembly of PA into nanostructures creates a dense hydrocarbon-like microenvironment within an aqueous gel. The environment created locally upon assembly makes PA nanostructures and other self-assembling systems potentially ideal candidates for the delivery of hydrophobic or water-insoluble molecules in vivo.<sup>8</sup> Amphiphilic structures, such as block copolymers, anionic, and cationic surfactants, can sequester hydrophobic or lipid soluble organic molecules in aqueous solution during or after the self-assembly process.<sup>9</sup> The presence of a bioactive exposed molecule could be used for target-selective delivery of hydrophobic no-water soluble drugs.<sup>10</sup>

We have investigated the assembling properties of a PA molecule containing a dioctadecyl moiety as hydrophobic

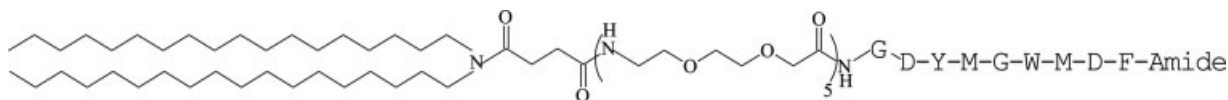


**FIGURE 1** Schematic representation of  $(C_{18}H_{37})_2-NCO(CH_2)_2CO(AdOO)_5-G-CCK8$  [(C18)<sub>2</sub>-L5CCK8] peptide amphiphile.

segment, a spacer consisting of a glycine residue and five units of 8-amino-3,6-dioxo-octanoic acid, and the carboxyl terminal sequence of the peptide hormone cholecystokinin, CCK8, as bioactive hydrophilic peptide. The molecule was designed considering that the hydrophobic dioctadecyl moiety should favor formation of stable aggregates, while the CCK8 peptide was selected for its potential use in biological recognition. In fact, CCK8 displays high affinity for both CCK<sub>1</sub> and CCK<sub>2</sub> cholecystokinin receptors.<sup>11</sup> These receptors have been often found overexpressed in several human tumors<sup>12</sup> and thus they represent potential targets for tumor diagnosis and for drug delivery: the <sup>111</sup>In radiolabel CCK8 analogue, [<sup>111</sup>In-DOTA]CCK8, bearing the chelating agent tetraazacyclodecane tetraacetic acid (DOTA) at the N-terminus of CCK8, is now in preclinical evaluation for scintigraphy of human medullary thyroid cancers overexpressing CCK receptors;<sup>13</sup> CCK8 functionalized macroaggregates have significant potential for selective delivery of drugs on a variety of cancerous tumors.

Here we described the synthesis of (C18)<sub>2</sub>L5CCK8 PA, schematized in Figure 1, and its self-assembling behavior in nanostructures at physiological pH. We also report on the structural properties of the nanostructures as resulting by Small-angle neutron scattering (SANS) studies and on the conformation of the amphiphilic peptide on the external surface of the aggregate as determined by CD spectroscopy. Finally, fluorescence experiments indicating the sequestration of pyrene, chosen as drug model, and of Doxorubicin within the nanostructures are reported. These studies provide helpful information to assess the use of this kind of supramolecular aggregates as potential carriers for selective delivery of hydrophobic, poor water-soluble drugs.

## EXPERIMENTAL METHODS

### Materials and Methods

Protected N<sup>α</sup>-Fmoc-amino acid derivatives, coupling reagents, and Rink amide MBHA resin were purchased from Calbiochem-Novabiochem (Laufelfingen, Switzerland). The Fmoc-8-amino-3,6-dioxo-octanoic acid (Fmoc-AdOO-OH) was purchased from Neosystem (Strasbourg, France). The N,N-dioctadecylsuccinamic acid was synthesized according to literature.<sup>14</sup> All other chemicals were commercially available by Sigma-Aldrich or Fluka (Buchs, Switzerland) or

LabScan (Stillorgan, Dublin, Ireland) and were used as received unless otherwise stated. All solutions were prepared by weight with doubly distilled water. The pH of all solutions was kept constant at 7.4 by using a 0.1 M phosphate buffer solution.

### Chemical Synthesis

Solid phase peptide synthesis was performed on a Shimadzu (Kyoto, Japan) Model SPPS-8 fully automated peptide synthesizer. Analytical RP-HPLCs were carried out on a Shimadzu 10A-LC using a Phenomenex C18 column (Torrance, CA), 4.6 × 250 mm, eluted with H<sub>2</sub>O/0.1% TFA (A) and CH<sub>3</sub>CN/0.1% TFA (B) mixture. In the analytical method two gradients from 60 to 80% B over 10 min at 1.0 ml/min flow rate and from 80 to 95% B over 15 min at 1.0 ml/min flow rate were used. Preparative RP-HPLCs were carried out on a Waters (Milford, MA) model Delta Prep 4000 equipped with a UV λ-Max Model 481 detector using a Vydac C18 column (Columbia, MD), 22 × 250 mm, eluted with the H<sub>2</sub>O/0.1% TFA (A) and CH<sub>3</sub>CN/0.1% TFA (B) mixture previously described and a linear gradient at 20 ml/min flow rate. Mass spectra were carried out on a MalDI-tof Voyager-DE Perceptive Biosystem (Framingham, MA) apparatus using the α-cyano-4-hydroxycinnamic acid as matrix and bovine insulin as internal reference.

$(C_{18}H_{37})_2-NCO(CH_2)_2CO(AdOO)_5-G-CCK8$  [(C18)<sub>2</sub>L5CCK8]. The (C18)<sub>2</sub>L5CCK8 synthesis was carried out in solid-phase under standard conditions using Fmoc strategy.<sup>15</sup> Rink-amide MBHA resin (0.78 mmol g, 1 mmol scale, 1.28 g) was used. The peptide chain was elongated by sequential coupling and Fmoc deprotection of the Fmoc-amino acid derivatives. All couplings were performed twice for 1 h, by using an excess of 4 equivalents for the single amino acid derivative. The α-amino acids were activated *in situ* by the standard HOBt/PyBop/DIPEA procedure. DMF was used as a solvent. Fmoc deprotection was carried out by 20% solution of piperidine in DMF after the coupling of each amino acidic residue. When the Gly-CCK8 synthesis was complete, the Fmoc N-terminal protecting group was removed and five residues of Fmoc-AdOO-OH were added. They were condensed to the α-NH<sub>2</sub> of the glycine residue in successive single couplings. An excess of two equivalents of Fmoc-AdOO-OH, PyBop, and HOBt and four equivalents of DIPEA were dissolved in DMF and added to the manual vessel. When all five linkers were coupled on the peptide chain, the N,N-dioctadecylsuccinamic acid, was bonded. The coupling was carried out by an excess of four equivalents (2.48 g, 4.0 mmol) of the lipophilic compound dissolved in 10 ml of DMF/DCM (50/50) mixture. 2.080 g (4.0 mmol) of PyBop, 0.612 g (4.0 mmol) of HOBt and 1.34 ml (8.0 mmol) of DIPEA, dissolved in DMF were introduced in the vessel like activating agents. The coupling time was 1 h under N<sub>2</sub> flow at room temperature. Yield for aliphatic acid coupling, monitored by the Kaiser test, was in the range 95–98%. For deprotection and cleavage, the fully protected resin was treated with a mixture of trifluoroacetic acid (TFA), triisopropylsilane (TIS), ethanedithiol

(EDT), and water in the TFA/TIS/EDT/H<sub>2</sub>O 93/2/2.5/2.5 ratio, and the free product precipitated at 0°C by adding water drop wise. Purification of the crude mixture was carried out by RP-HPLC ( $\lambda = 280$  nm),  $R_t = 26.2$  min. The final product was recovered at purity higher than 95% and with a final yield of 15%. Mass spectrum confirms the product identity (MW = 2243,  $m/z = 2244$ ).

### Preparation of the Solutions

Stock solutions of PA were prepared in 0.1M phosphate buffer at pH 7.4, filtered through a 0.45  $\mu\text{m}$  filter. Concentrations of all solutions were determined by absorbance on a UV-vis Jasco (Easton, MD) Model 440 spectrophotometer with a path length of 1 cm using a molar absorptivity ( $\epsilon_{280}$ ) of  $6845\text{M}^{-1}\text{cm}^{-1}$  for CCK8. This value was calculated according to the Edelhoch method,<sup>16</sup> taking into account contributions from tyrosine and tryptophan present in the primary structure, which amount to  $1215$  and  $5630\text{M}^{-1}\text{cm}^{-1}$ , respectively.<sup>17</sup>

### Small-Angle Neutron Scattering

SANS measurements were performed at 25°C at the FRJ-2 research reactor in Jülich (Germany), with the KWS2 spectrometer. Neutrons with average wavelength of 6.3 Å and wavelength spread  $\Delta\lambda/\lambda < 0.1$  were used. Neutrons scattered from the samples were detected by a 2D arrays detector at two different sample-detector distances, (2 and 8 m), to get scattering cross sections in a range of the scattering vector modulus  $q$ , defined as  $q = 4\pi/\lambda \sin(\theta/2)$  with  $\theta$  scattering angle, comprised between 0.0053 and 0.16 Å<sup>-1</sup>. Samples, prepared by weight using D<sub>2</sub>O as solvent, were contained in 1 mm path length quartz cells, and measurement times ranged between 15 min and 2 h. The data were then corrected for background, empty cell, and solvent contributions and then reduced to absolute scattering cross sections, by using a Plexiglas sample as standard.<sup>18</sup>

### Atomic Force Microscopy

The AFM (Digital Instruments Nanoscope IIIa) was equipped with a sharpened silicon tip with a radius less than 5 nm. Samples were obtained dispersing the aggregates in acetone or ethanol diluted solutions and depositing 20–30  $\mu\text{l}$  of such solutions on a mica substrate. Images of the surface profiles were obtained by operating the AFM in the tapping mode, with a scan size and rate of 3  $\mu\text{m}$  and 2 Hz, respectively.

### Circular Dichroism Experiments

Far-UV CD spectra were collected at room temperature on a Jasco Model J-715 spectropolarimeter using 1 mm path length quartz cells. Other experimental settings were: scan speed, 10 nm/min; sensitivity, 50 mdeg; time constant, 16 s; bandwidth, 3 nm. Circular dichroism measurements were conducted on G-CCK8 and PA solutions at concentrations of  $1 \times 10^{-4}\text{M}$  in 2.5 mM phosphate buffer at pH 7.4. The CD spectra were collected from 260 to 195 nm, corrected for blank and adjusted for dilution.

### Fluorescence Studies

Critical micellar concentration (cmc) values and an evaluation of pyrene and Doxorubicin encapsulation were obtained by fluores-

cence spectroscopy using 1 cm path length quartz cell. Emission spectra were recorded at room temperature using a Jasco Model FP-750 spectrofluorimeter. Equal excitation and emission bandwidths were used throughout experiments, with a recording speed of 125 nm/min and automatic selection of the time constant. The cmc of PA was measured by using 8-anilino-naphthalene-1-sulfonate (ANS) as fluorescent probe. Small aliquots of a self-assembled aggregate solution ( $1 \times 10^{-4}\text{M}$ ) were added to a fixed volume of  $1 \times 10^{-5}\text{M}$  ANS dissolved in the same buffer. The cmc was determined by linear least-squares fitting of the fluorescence emission at 480 nm, upon excitation at 350 nm versus the amphiphile concentration as previously reported.<sup>19,20</sup> Pyrene and Doxorubicin encapsulation in PA were evaluated by titration experiments. The excitation wavelength of pyrene and Doxorubicin were settled at 335 and 480 nm, respectively. Small amount of stock solutions of  $2.0 \times 10^{-4}\text{M}$  pyrene in ethanol in 2.5 mM phosphate buffer containing 0.9% wt NaCl, were added to  $1.0 \times 10^{-4}\text{M}$  solution of PA or to pure water. The repartition coefficient between Doxorubicin in PA solution/Doxorubicin in water was evaluated by a fluorescence titration of PA in  $8.6 \times 10^{-7}\text{M}$  of Doxorubicin solution.

## RESULTS AND DISCUSSION

The self-assembling PA (C18)<sub>2</sub>L5CCK8 was synthesized by solid-phase methods using Rink-amide MBHA resin as polymeric support and the Fmoc/tBu chemistry. The CCK8 peptide was synthesized according to standard SPPS protocols.<sup>15</sup> At the Asp N-terminal residue of the CCK8 peptide a glycine residue and five units of 8-amino-3,6-dioxaoctanoic acid, acting as spacers, were consecutively added. After the Fmoc protecting group removal from the last ethoxylic spacer, the N,N-dioctadecylsuccinamic acid was coupled on the free NH<sub>2</sub> terminus. The product, purified by preparative RP-HPLC, was isolated in a 15% yield. Analytical data (Malditof mass spectrum and RP-HPLC) confirm the compound identity and its high purity. The self-assembling behavior of (C18)<sub>2</sub>L5CCK8 was characterized by cmc measurements, CD spectroscopy, and AFM images. The cmc value was determined by a fluorescence-based method using ANS as probe. The fluorescence intensity at 480 nm, corresponding to the maximum of spectrum, as a function of the PA concentration is reported in Figure 2a. The break-point indicates a cmc value of  $2 \times 10^{-6}\text{mol kg}^{-1}$  that confirms the high stability of the resulting supramolecular aggregates.

In Figure 2b a comparison of the circular dichroism (CD) spectra of the G-CCK8 nonapeptide and of the (C18)<sub>2</sub>L5CCK8 PA, above its cmc value, is reported. The G-CCK8 peptide assumes a random-coil conformation as well expected for a short peptide sequence.<sup>21</sup> In contrast, PA shows a large negative maximum at 218 nm, corresponding to a  $\beta$ -sheet structural motif due to the self-assembling of PA in nanostructures, driven by the interactions of the hydrophobic chains in the inner core and by the peptide side chains in the hydro-

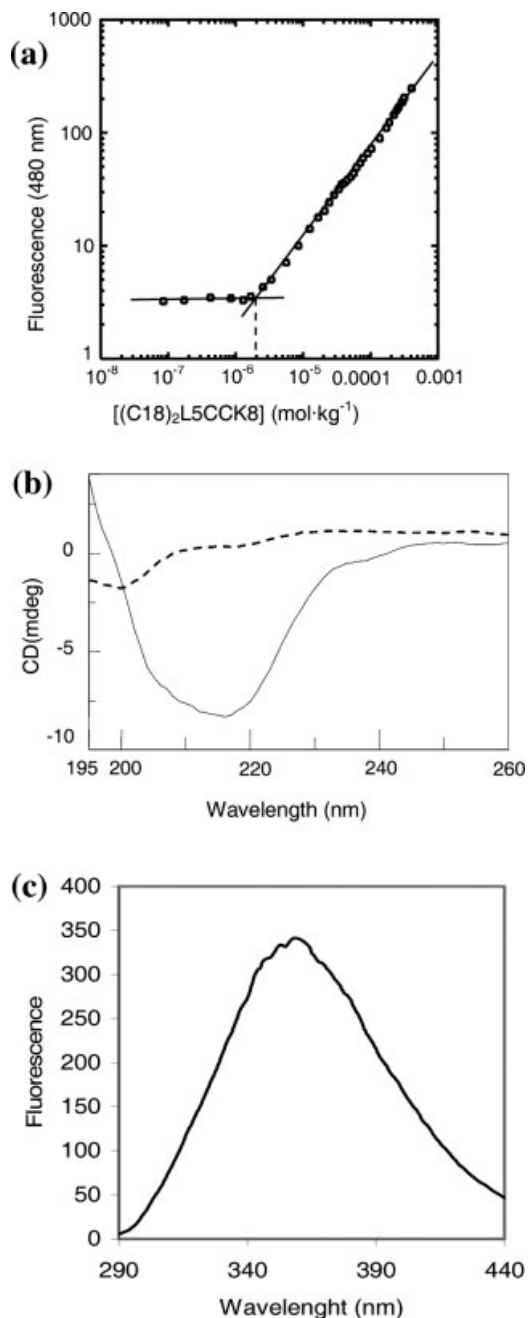


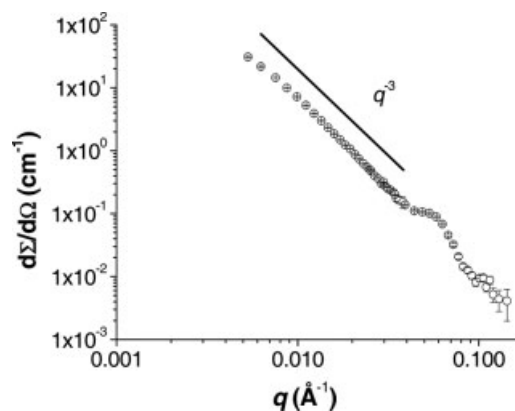
**FIGURE 2** (a) Fluorescence intensity of ANS fluorophore at 480 nm versus PA concentration. Cmc value ( $2 \times 10^{-6} \text{ mol kg}^{-1}$ ) is established from graphical break-point; (b) CD spectra of  $1.0 \times 10^{-4} \text{ M}$  G-CCK8 nonapeptide (—) and  $1.0 \times 10^{-4} \text{ M}$  (C18)<sub>2</sub>L5CCK8 peptide amphiphile (---) in 0.1M phosphate buffer at pH 7.4; (c) Fluorescence spectrum of tryptophan residue in  $1.0 \times 10^{-4} \text{ M}$  (C18)<sub>2</sub>L5CCK8 peptide amphiphile. The spectrum was excited at 280 nm.

philic shell.<sup>22</sup> The presence of the peptide moiety in the hydrophilic external shell is confirmed by the presence of a fluorescence maximum at 360 nm that is diagnostic of the

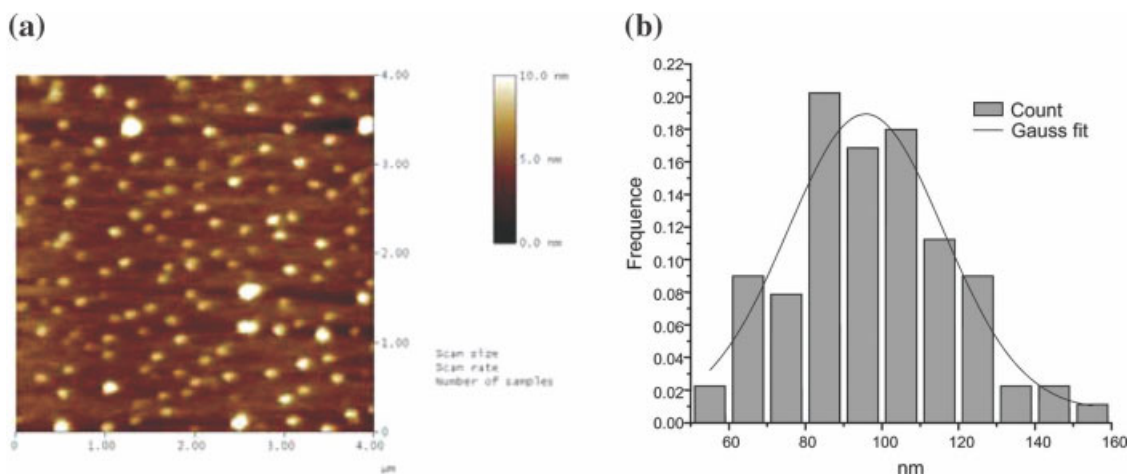
hydrophilic environment of the indole group on tryptophan side-chain (Figure 2c).<sup>23</sup> Tryptophan exposition on the hydrophilic shell of the aggregate suggests the bioavailability of CCK8 peptide to the receptor binding site.

Figure 3 reports the absolute scattering cross sections  $d\Sigma/d\Omega$  obtained for the binary system (C18)<sub>2</sub>L5CCK8-D<sub>2</sub>O ( $c = 8.1 \times 10^{-4} \text{ mol kg}^{-4}$ ). From the inspection of the SANS pattern it is possible to highlight the presence of a two-scale structure. The shoulder occurring in the region for which  $q > 0.03 \text{ \AA}^{-1}$ , can be ascribed to the scattering of relatively small aggregates (micelles), i.e. formed by the aggregation of (C18)<sub>2</sub>L5CCK8 molecules, that expose the hydrophilic moieties toward the outer solvent, preserving the hydrophobic alkylic chains from the D<sub>2</sub>O. The increase of the cross section at lower  $q$  ( $q < 0.03 \text{ \AA}^{-1}$ ) is caused by an upper level structure. In general, if we consider a fractal object with a fractal dimension  $D$ , the scattering cross section scales with a power law  $d\Sigma/d\Omega \propto q^{-D}$ . In our case, the exponent  $D = 3$  observed in Figure 3 indicates that in the region  $q < 0.03 \text{ \AA}^{-1}$  the arrangement observed resemble a 3D structure.<sup>24</sup> Since, no Guinier regime is observed in the  $q$  range spanned by SANS measurements, it is possible to conclude that linear dimensions of this upper level structure is at least  $2\pi/q_{\text{min}} = 100 \text{ nm}$ . Indeed, the AFM image of aggregates at high magnification, reported in Figure 4a, revealed nanostructures with an average size of bright spots ( $96 \pm 20 \text{ nm}$ ).

The encapsulation of pyrene, a fluorophoric compound chosen as drug model, in the PA nanostructure was investigated in phosphate buffer solution. Pyrene presents a very low water solubility ( $2.5 \times 10^{-5} \text{ M}$ ), but its solubility strongly increases in nanostructure containing water solutions because of its entrapment in the hydrophobic core of the nanostructure obtained by PA aggregation.<sup>8</sup> The entrapment process has been studied by comparing the fluorescence spec-



**FIGURE 3** Scattering cross sections obtained at 25°C for a solution  $8.1 \times 10^{-4} \text{ mol kg}^{-1}$  of the (C18)<sub>2</sub>L5CCK8 peptide amphiphile.



**FIGURE 4** (a) AFM image of PA aggregates at  $1 \times 10^{-5} \text{ mol kg}^{-1}$ ; (b) Diameter histogram distribution for aggregates.

tra of pyrene in water solution and in  $1.0 \times 10^{-4} \text{ M}$  PA containing solution, both buffered at pH 7.4. In both solutions increasing amounts of pyrene (from  $6.0 \times 10^{-7}$  to  $1.8 \times 10^{-5} \text{ M}$ ) were added, following the titration by recording fluorescence spectra (titrations are reported in Figure 5). The fluorescence emission spectrum of pyrene shows vibrational bands that are affected by the polarity of the surrounding environment of the probe molecules. Specifically, changes in the relative intensity of the first ( $I_1$  at 373 nm) and the third ( $I_3$  at 393 nm) vibrational bands in the pyrene emission spectrum have been proven to be reliable tools in examining the polarity of the microenvironment.<sup>25</sup> Moreover, the fluorescence emission at 480 nm is diagnostic for excimer formation within the nanostructures.<sup>8</sup> Both the relative intensity variation of the bands at 373 and 393 nm ( $I_1/I_3$  changes from 1.11 to 0.85) observed by comparing the titration in absence and in presence of PA, as well the appearing of the 480 nm band by adding pyrene to PA containing water solution, indicate the entrapment of pyrene in the inner hydrophobic region of the PA nanostructures.

To rule out the occurrence of several interactions of pyrene molecule with the ethoxylic spacers interposed between hydrophobic chains and the bioactive CCK8 peptide in PA molecule, additional fluorescence control experiments were carried out. We found that fluorescence titration of pyrene in  $1.0 \times 10^{-4} \text{ M}$  solution of PEG-600 (chosen for its similar length to five ethoxylic AdOO linkers) is comparable with pyrene titration in water solution. Moreover, similar experiments were also carried out by using a  $1.0 \times 10^{-4} \text{ M}$  of CCK8 or amphiphilic compound at concentration below its cmc, in water solution, to exclude pyrene interaction with the octapeptide fragment and with PA in non aggregated form, respectively. The results indicate that the variation of fluores-

cence emission spectra of pyrene could be only attributed to the incorporation of the fluorophore in already formed PA nanostructures.

We have also investigated the efficiency of PA nanostructures in loading anticancer molecules, such as the cytotoxic drug Doxorubicin, in their inner compartment. Fluorescence

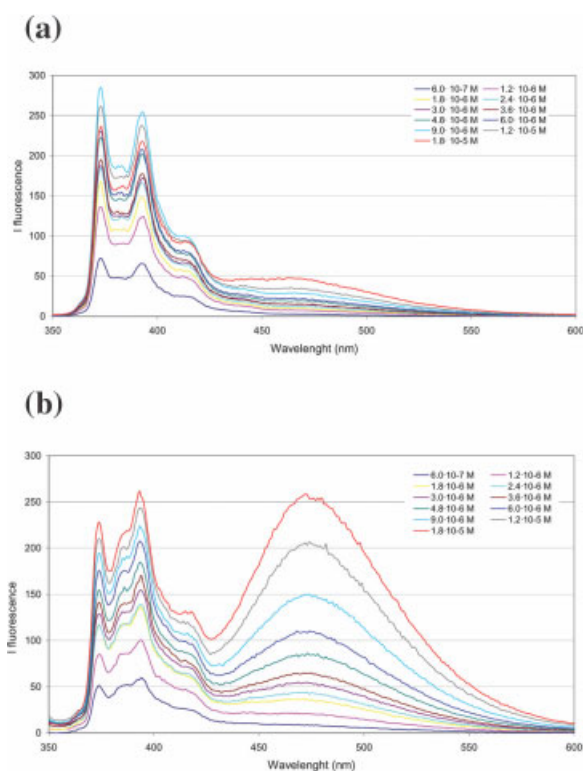


**FIGURE 5** (a) Fluorescence titration of pyrene in water solution and in (b)  $1.0 \times 10^{-4} \text{ M}$  peptide amphiphile containing solution, both buffered at pH 7.4. Different amounts of pyrene, from  $6.0 \times 10^{-7}$  to  $1.8 \times 10^{-5} \text{ M}$ , as final concentration, are added.

titration of PA was carried out on a  $8.6 \times 10^{-7} M$  Doxorubicin containing solution, buffered at pH 7.4. As already reported,<sup>26</sup> the fluorescence intensity of Doxorubicin, as well as the other molecules belonging to the anthracycline family, increases when it is encapsulated in nanostructure: in fact the hydrophobic environment avoids the dynamic quenching because of collisions with water molecules.

Fluorescence measurements allowed extracting the value of the partition constant  $K_r$  defined according to Eq. (1)

$$K_r = \frac{[D]_{(PA)}}{[D]_{(w)}} \quad (1)$$

where  $[D]_{(PA)}$  and  $[D]_{(w)}$  are the concentration of Doxorubicin in the inner compartment of PA aggregates and in the external water, respectively. To evaluate  $K_r$ , a titration of a  $8.6 \times 10^{-7} M$  Doxorubicin solution with increasing amounts of PA has been performed. Fluorescence intensity at 590 nm has been recorded as a function of PA concentration  $I_{590}(c_{PA})$ . Fluorescence intensity  $\bar{I}_{590}$  for a solution of Doxorubicin in water at the same concentration used for the titration ( $8.6 \times 10^{-7} M$ ) has also been measured. From these values it is possible to evaluate the molar fraction of Doxorubicin  $x_D(c_{PA})$  dissolved in the hydrophobic environment, according to Eq. (2)

$$x_D(c_{PA}) = \frac{n_{(PA)}}{n_{(PA)} + n_{(w)}} \quad (2)$$

where  $n_{(i)}$  represents the moles of Doxorubicin dissolved in the phase  $i$ .  $x_D(c_{PA})$  is correlated to the fluorescence intensities through the relation

$$x_D(c_{PA}) = \frac{I_{590}(c_{PA}) - \bar{I}_{590}}{I_{590}^\infty - \bar{I}_{590}} \quad (3)$$

where  $I_{590}^\infty$  is the limit fluorescence intensity of Doxorubicin, obtainable through an extrapolation of fluorescence intensities  $I_{590}(c_{PA})$ . Algebraic manipulations allow correlating  $K_r$  with  $x_D(c_{PA})$

$$\frac{1}{x_D(c_{PA})} = 1 + \frac{1}{K_r} \left( \frac{1}{\phi(c_{PA})} - 1 \right) \quad (4)$$

where  $\phi$  is the fraction volume of the hydrophobic aggregates.

The volume fraction  $\phi$  is obtained from the stoichiometric concentration  $C$  of the PA molecules. Volume fraction  $\phi$  is defined as the ratio between the volume of all the PA aggregates  $V_{PA}$  and the volume of the system  $V$

$$\phi = \frac{V_{PA}}{V} \quad (5)$$

Volume  $V_{PA}$  can be written as the product of the molecular volume  $v_{PA}$  of PA (estimated in  $\sim 3000 \text{ \AA}^3$ ) and the number of PA molecules present in the system as micelles  $N_{PA}$

$$\phi = \frac{v_{PA} N_{PA}}{V} \quad (6)$$

But the ratio  $N_{PA}/V$  can be identified as the concentration of PA monomers present in the micelles  $c_{PA}^*$

$$\phi = \frac{v_{PA} N_{PA}}{V} = v_{PA} L_A c_{PA}^* \quad (7)$$

In turn  $c_{PA}^*$  can be written as the difference between the stoichiometric PA concentration  $C$  and the critical micellar concentration  $cmc$

$$\phi = \frac{v_{PA} N_{PA}}{V} = v_{PA} L_A c_{PA}^* = v_{PA} L_A (C - cmc) \quad (8)$$

from which the volume fraction  $\phi$  is readily calculated. Thus, by plotting  $1/x_D$  vs.  $1/\phi - 1$  the partition constant, as the reciprocal of the angular coefficient of the fit line, is obtained. Figure 6 reports the reciprocal of the molar fraction of Doxorubicin dissolved in the hydrophobic environment vs.  $1/\phi - 1$ , along with the line that has been fit to the experimental data. From the fitting procedure it has been obtained for  $K_r$  the value  $(5.0 \pm 0.5) \times 10^5$ , that indicates a strong preference of Doxorubicin for the inner hydrophobic environment of PA structures.

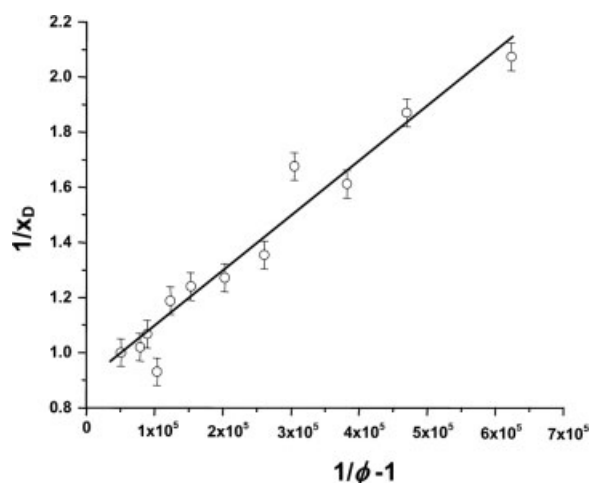


FIGURE 6 Reciprocal of the molar fraction  $x_D$  of Doxorubicin dissolved in the hydrophobic environment of PA aggregates vs.  $1/\phi - 1$ , along with the line fit to the experimental data.

## CONCLUSIONS

(C18)<sub>2</sub>L5CCK8 PA is able to self-assemble spontaneously in well-ordered nanostructures in aqueous solution. These nanostructures, fully characterized by structural measurements, are able to encapsulate poorly water soluble molecules such as pyrene and Doxorubicin in their hydrophobic compartment. The encapsulation process can be followed and quantified by fluorescence technique. The reported PA supramolecular aggregates could be employed for target selective drug delivery of hydrophobic drugs on a biological target, through the bioactive peptide exposed on the external surface. In fact, the bioactive CCK8 peptide exposed on the external surface of the nanostructures could interact with cholecystokinin receptors overexpressed by cancer cells. In this way the entrapped drug is mainly delivered in proximity of the tumor, thus reducing the well-expected toxic side effects on non-target organs.

One of us (G. Man.) thanks the Institut für Festkörperforschung des Forschungszentrums Jülich for the provision of beam time, and Dr. Aurel Radulescu for his support at the KWS2 instrument.

## REFERENCES

- Hartgerink, J. D.; Beniash, E.; Stupp, S. I. *Science* 2001, 294, 1684–1688.
- Hartgerink, J. D.; Beniash, E.; Stupp, S. I. *Proc Natl Acad Sci USA* 2002, 99, 5133–5138.
- Niece, K. L.; Hartgerink, J. D.; Donners, J. J. M.; Stupp, S. I. *J Am Chem Soc* 2003, 125, 7146–7147.
- Silva, G. A.; Czeisler, C.; Niece, K. L.; Beniash, E.; Harrington, D. A.; Kessler, J. A.; Stupp, S. I. *Science* 2004, 303, 1352–1355.
- Behanna, H. A.; Donners, J. J. M.; Gordon, A. C.; Stupp, S. I. *J Am Chem Soc* 2005, 127, 1193–1200.
- Accardo, A.; Tesaro, D.; Roscigno, P.; Gianolio, E.; Padano, L.; D'errico, G.; Pedone, C.; Morelli, G. *J Am Chem Soc*, 2004, 126, 3097–3107.
- Pajewski, R.; Ferdani, R.; Pajewska, J.; Djedovic, L.; Schlesinger, P. H.; Gokel, G. W. *Org Biomol Chem* 2005, 3, 619–625.
- Guler, M. O.; Claussen, R. C.; Stupp, S. I. *J Mater Chem* 2005, 15, 4507–4512.
- Torchilin, V. P. *Cell Mol Life Sci* 2004, 61, 2549–2559.
- Nasongkla, N.; Shuai, X.; Ai, H.; Weinberg, B. D.; Pink, J.; Boothman, D. A.; Gao, J. *Angew Chem Int Ed* 2004, 43, 6323–6327.
- Wank, S. A. *Am J Physiol* 1995, 269, G628–G646.
- Reubi, J. C.; Schaer, J. C.; Waser, B. *Cancer Res* 1997, 57, 1377–1386.
- Kwekkeboom, D. J.; Bakker, W. H.; Kooij, P. P.; Erion, J.; Srinivasan, A.; de Jong, M.; Reubi, J. C.; Krenning, E. P. *Eur J Nucl Med* 2000, 27, 1312–1317.
- Schmitt, L.; Dietrich, C. *J Am Chem Soc* 1994, 116, 8485–8491.
- Chang, W. C.; White, P.D. In *Fmoc Solid Phase Peptide Synthesis*, Oxford University Press: New York, 2000.
- Edelhoch, H. *Biochemistry* 1967, 6, 1948–1954.
- Pace, C. N.; Vajdos, E.; Fee, L.; Grimsley, G.; Gray, T. *Protein Sci* 1995, 4, 2411–2423.
- Wignall, G. D.; Bates, F. S. *J Appl Crystallogr* 1987, 20, 28–40.
- Birdi, K. S.; Singh, H. N.; Dalsager, S. U. *J Phys Chem* 1979, 83, 2733–2737.
- De Vendittis, E.; Palumbo, G.; Parlato, G.; Bocchini, V. *Anal Biochem* 1981, 115, 278–286.
- Underfriend, S.; Meienhofer, J. In *The Peptides*, Vol. 7, Hruby, V. J. Ed.; Academic press: New York, 1985.
- Claussen, R. C.; Rabatic, B. M.; Stupp, S. I. *J Am Chem Soc* 2003, 125, 12680–12681.
- Permyakov, E. A. *Luminescent Spectroscopy of Proteins*; CRC Press: Boca Raton, FL, 1993.
- Schmidt, P. W. In *Some Fundamental Concepts and Techniques Useful in Small-Angle Scattering Studies of Disordered Solids in Modern Aspects of Small-Angle Scattering*; Brumberger, H., Ed.; Kluwer Academic: Boston, 1995.
- Nakajima, A. *J Lumin* 1976, 11, 429–432.
- Rapoport, N.; Pitina, L. *J Pharm Sci* 1998, 87, 321–325.